Effect of Black Hole Spin on Christodoulou Memory

Ashok Choudhary* and Sean T. McWilliams†
Department of Physics and Astronomy, West Virginia University, Morgantown, WV 26506, USA

The Christodoulou memory, which is a nonlinear memory effect sourced by the gravitational wave stress tensor, produce a growing, nonoscillatory change in the gravitational wave "plus" polarization. This results in the permanent displacement of a pair of freely falling test masses after the gravitational wave has passed. While the memory contribution during early in-spiral is well described by Post-Newtonian approximation, the contribution at merger must be obtained from Numerical relativity simulations. The Post-Newtonian corrections upto 3PN order to the gravitational wave memory for quasicircular, inspiralling compact binaries for non spinning has been computed by Favata et al.[Physical Review D 80, 024002 (2009)]. Here we include the Spin contribution at leading order and calculate the memory effect upto 3PN order. We also compute memory contribution at merger from Numerical relativity using Weyl curvature component ψ_4 after removing the unphysical low frequency contribution due to spectral leakage. We use the method described in [Class. Quantum Grav. 28 195015] for integration which control the amplification of the unphysical frequency resulting from spectral leakage.

I. INTRODUCTION

Gravitational wave memory effect results in a permanent displacement of test masses after the gravitational wave has passed through an "ideal" GW detector. There are two kinds of gravitational wave memory effects: linear and nonlinear. The linear memory is produced by gravitational sources that produce a net change in the time derivative of one or more of their source-multipole moments. At leading order in a Post-Newtonian (PN) expansion, the linear memory causes a net change in the GW field given by

$$\Delta h^{TT}_{jk} = \frac{2}{R}\Delta\left(\ddot{I}^{TT}_{jk}\right) \tag{1.1}$$

where I_{ij} is the source mass-quadrupole moment, R is the distance to the source and Δ describes the net change in the quantity from early to late times. Gravitational waves with linear memory are important in case of unbound systems and have been studied studied in context of supernova explosion, asymmetric mass loss due to neutrino emission and gamma-ray-burst jets, [1–3]

The linear memory produced by a system of N bodies with changing mass M_A or velocities V_A is given by the following general formula for by Thorn [4]

$$\Delta h^{TT}_{jk} = \Delta\sum_{A=1}^{N}\frac{4M_A}{R\sqrt{1-v_A^2}}\left[\frac{v_A^j v_A^k}{1-\boldsymbol{v}_A\cdot\boldsymbol{N}}\right] \tag{1.2}$$

where the masses are unbound in their initial and final states(or both). Here Δ refers to take difference between the final and initial values of the summations, and $\boldsymbol{N}$ is the unit vector that points from the source to the observer.
The other kind of memory is the nonlinear memory, which is also called Christodoulou memory. This was independently discovered by Christodoulou [5], Payne [6], Blanchet and Damour [7].

Christodoulou arises from a change in the radiative multiple moment that is sourced by the energy flux of the radiated gravitational wave. It can be understood in the following way. Consider the Einstein field equation in harmonic gauge. [8]

$$\Box\bar{h}^{\alpha\beta} = -16\pi(-g)(T^{\alpha\beta}+t^{\alpha\beta}_{LL}) - \bar{h}^{\alpha\mu}_{,\nu}\bar{h}^{\beta\nu}_{,\mu} + \bar{h}^{\mu\nu}\bar{h}^{\alpha\beta}_{,\mu\nu} \tag{1.3a}$$

$$\bar{h}^{\alpha\beta}{}_{,\beta} = 0 \tag{1.3b}$$

where

$$\bar{h}^{\alpha\beta} = \eta^{\alpha\beta} - \sqrt{-g}g^{\alpha\beta} \tag{1.4}$$

is the gravitational field tensor, g is the determinant of the metric $g_{\alpha\beta}$, $T^{\alpha\beta}$ is the matter stress-energy tensor, $t^{\alpha\beta}_{LL}$ is the Landau-Lifshitz pseudotensor, $\Box \equiv -\partial_t^2 + \nabla^2$ is the flat-space wave operator, a comma denotes a partial derivative ($_{,\mu} \equiv \partial_\mu$), and ∇^2 is a flat-space Laplace operator. The Landau-Lifshitz term is the Gravitational wave stress tensor [9].

$$T^{gw}_{jk} = \frac{1}{32\pi}\langle h^{TT}_{ab,j}h^{TT}_{ab,k}\rangle \approx T^{gw}_{00}n_j n_k = \frac{1}{R^2}\frac{dE^{gw}}{dtd\Omega}n_j n_k \tag{1.5}$$

where $\frac{dE^{gw}}{dtd\Omega}$ is the GW energy flux, n_j is a unit radial vector, the angle-bracket mean to average over several wavelengths, $h^{TT}_{ab} = \bar{h}^{TT}_{ab}$. When we apply standard Green's function to right hand side of equation 1.3a, we obtain the following correction term to GW field [10]

$$\delta h^{TT}_{jk} = \frac{4}{R}\int_{-\infty}^{T_R}dt'\left[\frac{dE^{gw}}{dt'd\Omega'}\frac{n'_j n'_k}{(1-\boldsymbol{n'}\cdot\boldsymbol{N})}d\Omega'\right]^{TT} \tag{1.6}$$

where T_R is the retarded time. This equation shows that part of the distant GW is sourced by loss of GW energy. The nonlinear memory occurs in any system that radiates GWs. These systems are usually considered to have a vanishing linear memory. The nonlinear memory [Eq.1.6] can be described by equation 1.2, the formula for the linear memory if the unbound object in the system are taken to be the individual gravitons with energy $E_A = M_A/(1-v_A^2)^{1/2}$ and velocities $v_A^j = c\,n'^j_A$.[11]

The Christodoulou memory is an interesting consequence of the nonlinearity of general relativity, it arises from the loss of GW energy from the system and the effect of this loss on the system's

*Electronic address: aschoudhary@mix.wvu.edu
†Electronic address: sean.mcwilliams@mail.wvu.edu

radiative mass multipole moments. The nonlinear memory effect arises from nonlinear interactions at 2.5 PN order but affects the gravitational waveform at leading (0PN) order. This memory effect causes a non oscillatory shift in the amplitude of + polarization, which starts at early times and slowly grows during the inspiral. The PN waveform allow us to model the slow growth of memory during the inspiral phase of coalescence, but the most contribution to this nonlinear memory come from the merger phase where the PN model do not work. In this case the memory must be extracted from Numerical relativity simulations. However, it is quite challenging to extract the nonlinear memory accurately from numerical simulations of binary black holes. Numerical relativity simulations can most accurately compute the $(l, m) = (2, 2)$ mode of the waveform; but the nonlinear memory is present in only $m = 0$ mode. These $m = 0$ modes tend to be much smaller in magnitude and depends more sensitively on initial conditions than other modes. For detailed discussion on this see section V in reference [12]

The NR simulations mostly easily compute the curvature scalar Ψ_4 and decompose its values at large R into a sum over spin-weighted spherical harmonic modes:

$$\Psi_4 = \ddot{h}_+ - i\ddot{h}_\times = \sum_{l=2}^{\infty}\sum_{m=-l}^{l} \psi_{lm}(t,R)\,{}_{-2}Y_{lm}(\Theta,\Phi) \tag{1.7}$$

In terms of the ψ_{lm} modes, the leading-order Christodoulou-memory modes are smaller than the ψ_{22} modes by $five$ PN orders.The relative mode magnitudes([12]) are $\psi_{22} \approx 690\psi_{20} \approx 4.5\times10^4\psi_{40}$ at $x \approx 1/5$. There are many other difficulties too in calculating memory from numerical relativity data. Construction of the h_{lm} from ψ_{lm} requires two integration constants to be specified. Choosing these integration constant to be zero [13] causes an artificial memory and a slope in the h_{lm} modes. This artificial memory is unphysical and arises from the finite size of the initial separation and extraction radius.The initial burst of junk radiation also contribute to artificial memory.

Numerical relativity simulations starts at a finite radius, so although it contains most part of gravitational wave memory, PN results should be used for early inspiral phase. The significance of memory accumulated during the inspiral phase can be seen by looking at the largest memory mode h_{20}. Consider the leading-(Newtonian)-order piece of the largest memory mode h_{20}:

$$h_{20}^{NR}(T_R) = \frac{1}{\sqrt{2}R}\int_{T_0}^{T_R} U_{20}^{(mem)(1)}(t)dt \tag{1.8}$$

where $U_{20}^{(mem)(1)}$ is given by the leading order piece of Eq. (3.13a) in ref [12], and the T_0 is the starting time of the simulation. For a realistic, quasicircular binary that inspirals from a large initial separation, $T_0 \to -\infty$. The NR simulations of binaries that starts at a finite initial separation would underestimate the size of the memory. For a simulation that starts with an initial separation of $10M$, the error in the memory at a harmonic coordinate separation of $5M$ is 50%.[12]

The corrections to the leading-oder formula for the nonlinear memory's contribution to 3PN order for non-spinning binaries has been computed by by Favata [12]. However the effect of binary spins have not been explored these results.(*Ashok:need to add why looking at spins is important*)

In this paper we calculate the nonlinear memory contribution to the + waveform polarization and look at the effect of spin contribution. In Sec. II, we describe the calculation required to compute memory contribution to the post-Newtonian waveform of quasi-circular, inspiralling binaries. In Sec. III, we describe the method used to extract memory contribution from NR simulations. Sec. IV we give the results which looks at the effect of spin on total nonlinear memory. We use PN expressions for memory for early time and for late time we use memory extracted from NR simulations.

II. MEMORY CONTRIBUTION TO POST-NEWTONIAN WAVEFORM POLARIZATION

The mode decomposition of gravitational wave polarization is given by

$$h_+ - ih_\times = \sum_{l=2}^{\infty}\sum_{m=-l}^{m=l} h^{lm}\,{}_{-2}Y^{lm}(\Theta,\Phi) \tag{2.1}$$

where ${}_{-2}Y^{lm}$ are spin-weighted spherical harmonics, the angles (Θ,Φ) indicates the direction from the source to the observer. In a multipolar expansion of the GW field, the modes h^{lm} are related to the radiative mass U^{lm} and the current V^{lm} multipole via

$$h^{lm} = \frac{G}{\sqrt{2}\,R}\left[U^{lm}(T_R) - \frac{i}{c}V^{lm}(T_R)\right] \tag{2.2}$$

Here R is the distance from source to observer, T_R is retarded time. We assume $c = G = 1$ for all out calculations. The spin weighted spherical harmonics are defined in terms of the Wigner d function by

$${}_{-2}Y^{lm}(\Theta,\Phi) = (-1)^2\sqrt{\frac{2l+1}{4\pi}}d^l_{ms}(\Theta)e^{im\Phi} \tag{2.3}$$

Here

$$d^l_{ms} = \sqrt{(l+m)!(l-m)!(l+s)!(l-s)!} \tag{2.4}$$

$$\times\sum_{k=k_i}^{k_f}\frac{(-1)^k(\sin\frac{\Theta}{2})^{2k+s-1}(\cos\frac{\Theta}{2})^{1l+m-s-2k}}{k!(l+m-k)!(l-s-k)!(s-m+k)!} \tag{2.5}$$

where $k_i = \max(0, m-s)$ and $k_f = \min(l+m, l-s)$.
When the GW field is decomposed into spin-weighted spherical harmonic modes, the nonlinear memory can be shown to yield a correction to the radiative mass multipole moments that enters at 2.5PN and higher orders. For more detail about GW multipole expansion [8]. The correction to the radiative mass multipole moments is given by

$$U^{(mem)}_{lm} = 32\pi\frac{(l-2)!}{2(l+2)!}\int_{-\infty}^{T_R}dt\int d\Omega\frac{dE_{gw}}{dtd\Omega}(\Omega)Y^*_{lm}(\Omega) \tag{2.6}$$

The radiative current moments V_{lm} do not contribute to nonlinear memory. The GW energy flux can be computed from the GW stress-energy tensor and is given by [14]

$$\frac{dE_{gw}}{dtd\Omega} = R^2T^{gw}_{00} = \frac{R^2}{32\pi}\langle\dot{h}^{TT}_{jk}\dot{h}^{TT}_{jk}\rangle = \frac{R^2}{16\pi}\langle\dot{h}^2_+ + \dot{h}^2_\times\rangle \tag{2.7}$$

where the angled bracket mean to average over several wavelengths. The energy flux can be written in terms of h_{lm} modes using equation 2.1 in the following way:

$$\frac{dE_{gw}}{dtd\Omega} = \frac{R^2}{16\pi}\sum_{l'=2}^{\infty}\sum_{l''=2}^{\infty}\sum_{m'=-l'}^{l'}\sum_{m''=-l''}^{l''}\langle \dot{h}_{l'm'}\dot{h}^*_{l''m''}\rangle {}_{-2}Y^{l'm'}(\theta,\phi){}_{-2}Y^{l''m''*}(\theta,\phi) \tag{2.8}$$

The memory contribution to the mass multipole moment can now be evaluated using equation 2.6 and 2.8. The angular part of the integral has the following form

$$\int d\Omega {}_{-2}Y_{l'm'}(\theta,\phi){}_{-2}Y^*_{l''m''}(\theta,\phi)Y^*_{lm}(\theta,\phi) \tag{2.9}$$

The above integral can be evaluated as done in section III of Favata[12]. The results are also shown in appendix A. The time derivative of the memory mass-multipole moment is defines as $U^{(mem)(1)}_{lm} \equiv \frac{dU^{(mem)}_{lm}}{dT_R}$ [12], which when combined using equation 2.6 and 2.8 and Appendix A, can be written as

$$\begin{aligned} U^{(mem)(1)}_{lm} =& R^2\sqrt{\frac{2(l-2)!}{(l+2)!}}\sum_{l'=2}^{\infty}\sum_{l''=2}^{\infty}\sum_{m'=-l'}^{l'}\sum_{m''=-l''}^{l''}(-1)^{m+m'} \\ &\times\left\langle \dot{h}_{l'm'}\dot{h}^*_{l'm'}\right\rangle G^{2-20}_{l'm'lm'-m''-m} \end{aligned} \tag{2.10}$$

where $G^{2-20}_{l'm'lm'-m''-m}$ is the angular integral of equation 2.9 and is given in Appendix A. The above equation can be used to compute the first time derivative of mass-multipole moment by substituting the GW modes h_{lm}. When evaluating equation 2.10, we are only interested in $m = 0$ modes. The $m \neq 0$ terms yield oscillatory contribution to the waveform polarizations that enter at higher PN orders then the nonoscillatory, $m = 0$ terms. The non-vanishing, non-oscillatory modes are $U^{(mem)}_{l0}$ with l-even. These $U^{(mem)}_{l0}$ consist of time-integral of polynomials in $x \equiv (M\omega)^{2/3}$ (where ω is the orbital angular frequency), with each terms of the form

$$\int_{-\infty}^{T_R} x^n dt = \int_{-\infty}^{T_R}\frac{x^n}{\dot{x}}dx \tag{2.11}$$

After performing the change of variable indicated in above equation 2.11, evaluation of the resulting integrals requires a model for the frequency evolution of the binary. The adiabatic evolution of the frequency (or x) is easily derived from energy balance ($\mathcal{L}_{GW} = -\dot{E}$). and the relation $\dot{x} = -\mathcal{L}_{GW}/(dE/dx)$. The 3.5PN orbital energy and flux are given in Appendix C of reference [15]. Here we who only upto 1.5 PN terms, the complete expression are show in Appendix C1. The 1.5 PN expression for energy is given by

$$E = -\frac{\eta M x}{2}\left\{1 + x\left[-\frac{3}{4} - \frac{\eta}{12}\right] + x^{3/2}\left[\left(\frac{8}{3} - \frac{4\eta}{3}\right)\boldsymbol{\chi}_s\cdot\hat{\mathbf{L}}_N + \frac{8}{3}\delta\boldsymbol{\chi}_a\cdot\hat{\mathbf{L}}_N\right]\right\} \tag{2.12}$$

and the 1.5 PN GW luminosity is given by

$$\mathcal{L} = \frac{32}{5}\eta^2 x^5\left\{1 + x\left[-\frac{1247}{336} - \frac{35\eta}{12}\right] + x^{3/2}\left[4\pi - \left\{\left(\frac{11}{4} - 3\eta\right)\boldsymbol{\chi}_s\cdot\hat{\mathbf{L}}_N + \frac{11}{4}\delta\boldsymbol{\chi}_a\cdot\hat{\mathbf{L}}_N\right\}\right]\right\} \tag{2.13}$$

Substituting the above two equation into $\dot{x} = -\mathcal{L}_{GW}/(dE/dx)$, and expanding upto 1.5 PN gives the following expression.

$$\frac{dx}{dt} = \frac{64\,x^5\,\eta}{5}\left\{1 + x\left[-\frac{743}{336} - \frac{11\eta}{4}\right] + x^{3/2}\left[4\pi - \frac{113}{12}\delta\,\boldsymbol{\chi}_a\cdot\hat{\mathbf{L}}_N - \left(-\frac{113}{19} + \frac{19\,\eta}{3}\right)\boldsymbol{\chi}_s\cdot\hat{\mathbf{L}}_N\right]\right\} \tag{2.14}$$

The results upto 3.5 PN are shows in Appendix C. The equation 2.14 can be used to change the integration with respect to time into

integration with respect to x as shown in equation in 2.11. The expressions for h_{lm} whose first time derivatives appear equation 2.10 can be obtained from Ref[15]. The GW modes for precessing binaries with small inclination angle on nearly circular orbits through 1.5 PN order are given in section IV of ref [15]. Setting $\iota = 0, \alpha = \pi$ in equation 4.16 and 4.17 gives the result for non-precessing case. In that case the spins are aligned along z axis, so we set $\chi_a^x = \chi_s^x = \chi_a^y = \chi_s^y = 0$. We can now write the expression as

$$h_{lm} = (-1)^{m+1} \frac{(2M\eta v^2)}{D_L} \sqrt{\frac{16\pi}{5}} e^{im\psi} \hat{h}_{lm}, \tag{2.15}$$

and $\hat{h}_{lm}$ modes are given by

$$\hat{h}_{22} = 1 + x\left(-\frac{107}{42} + \frac{55\eta}{42}\right) + x^{3/2}\left(2\pi - \frac{4\,\delta\,\chi_a^z}{3} + \frac{4}{3}(-1+\eta)\chi_s^z\right) \tag{2.16a}$$

$$\hat{h}_{21} = \frac{i\delta}{3}\left[x^{1/2} - x\frac{3}{2\delta}(\chi_a^z + \delta\chi_s^z) + x^{3/2}\left(-\frac{17}{28} + \frac{5\eta}{7}\right)\right] \tag{2.16b}$$

$$\hat{h}_{32} = \frac{9}{8}\sqrt{\frac{5}{7}}\left[\frac{8}{27}x(1-3\nu) + \frac{32}{27}x^{3/2}\eta\chi_s^z\right] \tag{2.16c}$$

The remaining h_{lm} expressions does not contain spin terms and the complete expressions upto 3PN terms can be directly taken from Ref.[16] We show the h_{lm} expressions for positive m values, but the results for negative m values can be obtained by the relation, $h_{l,-m} = (-1)^l \bar{h}_{lm}$. This results is not in general true for precessing binaries, but it continues to hold true of non-precessing case. The time derivative of h_{lm} modes can be obtained by following the procedure shown in Appendix B. With these modes we use equation 2.10 to evaluate the first time derivative of the memory mass-multipole moment, which is further integrated using equation 2.11. The results after integration are show in next section.

A. RESULTS: MEMORY CONTRIBUTION TO THE POST-NEWTONIAN WAVEFORM OF QUASI-CIRCULAR, INSPIRALLING BINARIES

The memory contribution to the spin-weighted spherical-harmonic modes of the polarization waveform [Eq. 2.2]. These quantities are related via

$$h_{l0}^{(mem)} = \frac{\alpha}{\sqrt{2}R} U_{l0}^{(mem)} = 8\sqrt{\frac{\pi}{5}}\frac{\eta M x}{R}\hat{H}_{lm} \tag{2.17}$$

where we have followed the notation of Sec. 9 of Ref. [16]. The notational parameter α accounts for the two commonly used choices for the polarization triad

$$\alpha = \begin{cases} (+1) & \text{for the Kidder [17] convention} \\ (-1) & \text{for the Blanchet et al. [16] convention} \end{cases} \tag{2.18}$$

The results of polarization modes in terms of $\hat{H}_{l0}$ are:

$$\begin{aligned}
\hat{H}_{20} = \alpha\frac{5}{14\sqrt{6}}\Bigg\{ & 1 + x\left[-\frac{4075}{4032} + \frac{67\,\eta}{48}\right] + x^{3/2}\left[\left(\frac{7}{480} + \frac{27\,\delta}{10} - \frac{7\,\eta}{120}\right)\boldsymbol{\chi}_a\cdot\hat{\mathbf{L}}_N + \left(\frac{27}{10} + \frac{7\,\delta^3}{480} - \frac{2\,\eta}{15}\right)\boldsymbol{\chi}_s\cdot\hat{\mathbf{L}}_N\right] \\
& x^2\left[-\frac{151877213}{67060224} - \frac{123815\,\eta}{44352} + \frac{205\,\eta^2}{352} + \left(-\frac{163}{96} + \frac{161\,\eta}{24}\right)\boldsymbol{\chi}_a^2 + \left(-\frac{27\,\delta}{8} - \frac{\delta^3}{48}\right)\boldsymbol{\chi}_s\cdot\boldsymbol{\chi}_a + \left(-\frac{27}{16} - \frac{\delta^4}{96} - \frac{\eta}{12}\right)\boldsymbol{\chi}_s^2\right] \\
& x^{5/2}\left[-\frac{253\,\pi}{336} + \frac{253\,\pi\,\eta}{84} + \left\{\frac{631}{32256} + \frac{788471\,\delta}{84672} + \left(-\frac{5}{126} - \frac{991\,\delta}{1008}\right)\eta - \frac{311\,\eta^2}{2016}\right\}\boldsymbol{\chi}_a\cdot\hat{\mathbf{L}}_N\right. \\
& \left. + \left\{\frac{788471}{84672} - \frac{631\,\delta^3}{32256} - \left(-\frac{36509}{2646} + \frac{311\,\delta^3}{8064}\right)\eta + \frac{853\,\eta^2}{252}\right\}\boldsymbol{\chi}_s\cdot\hat{\mathbf{L}}_N\right] \\
& x^3\left[-\frac{4397711103307}{532580106240} + \left(\frac{700464542023}{13948526592} - \frac{205\,\pi^2}{96}\right)\eta + \frac{69527951\,\eta^2}{166053888} + \frac{1321981\,\eta^3}{5930496} - \left(-\frac{7\,\pi}{256} + \frac{275\,\pi\,\delta}{12}\right.\right. \\
& \left.\frac{7\,\pi\,\delta}{256}\right)\boldsymbol{\chi}_a\cdot\hat{\mathbf{L}}_N + \left\{-\frac{42787}{32256} + \frac{791\,\delta}{9216} + \frac{113\,\delta^2}{576} + \left(\frac{354035}{32256} - \frac{791\,\delta}{2304}\right)\eta - \frac{2533\,\eta^2}{128}\right\}\boldsymbol{\chi}_a^2 \\
& \left\{\frac{275\,\pi}{12} - \frac{7\,\pi\,\delta^3}{256} - \frac{56\,\pi\eta}{3} + \left(\frac{791}{9216} - \frac{47869\,\delta}{21504} - \frac{743\,\delta^3}{21504} + \frac{791\,\delta^4}{9216} + \left(-\frac{77}{192} + \frac{87269\,\delta}{2304} - \frac{11\,\delta^3}{256}\right)\eta + \frac{133\,\eta^2}{576}\right)\boldsymbol{\chi}_a\cdot\hat{\mathbf{L}}_N\right\}\boldsymbol{\chi}_s\cdot\hat{\mathbf{L}}_N \\
& \left.\left\{-\frac{47869}{43008} + \frac{791\,\delta^3}{9216} - \frac{743\,\delta^4}{43008} + \left(\frac{57677}{1792} - \frac{133\,\delta^3}{2304} - \frac{11\,\delta^4}{512}\right)\eta - \frac{15029\,\eta^2}{1152}\right\}\boldsymbol{\chi}_s^2\right]\Bigg\}
\end{aligned} \tag{2.19a}$$

$$\hat{H}_{40} = \alpha \frac{1}{504\sqrt{2}} \left\{ 1 + x\left[-\frac{180101}{29568} + \frac{27227\,\eta}{1056} \right] + x^{3/2}\left[\left(\frac{7}{40} + \frac{27\,\delta}{10} - \frac{7\,\eta}{10} \right) \boldsymbol{\chi}_a \cdot \hat{\mathbf{L}}_N + \left(\frac{27}{10} + \frac{7\,\delta^3}{40} + \frac{46\,\eta}{5} \right) \boldsymbol{\chi}_s \cdot \hat{\mathbf{L}}_N \right] \right.$$
$$x^{5/2}\left[-\frac{13565\,\pi}{1232} + \frac{13565\,\pi\,\eta}{308} + \left\{ \frac{379}{2688} - \frac{1457321\,\delta}{68992} + \left(-\frac{59}{336} + \frac{3094367\,\delta}{22176} \right)\eta - \frac{87\,\eta^2}{56} \right\} \boldsymbol{\chi}_a \cdot \hat{\mathbf{L}}_N \right.$$
$$\left. \left\{ -\frac{1457321}{68992} + \frac{379\,\delta^3}{2688} + \left(\frac{5892749}{38808} + \frac{87\,\delta^3}{224}\eta - \frac{469813\,\eta^2}{5544} \right) \right\} \boldsymbol{\chi}_s \cdot \hat{\mathbf{L}}_N \right]$$
$$x^2\left[\frac{2201411267}{158505984} - \frac{34829479\,\eta}{432432} + \frac{844951\,\eta^2}{27456} + \left(-\frac{85}{48} + 7\,\eta \right) \boldsymbol{\chi}_a^2 + \left(-\frac{27\,\delta}{8} - \frac{\delta^3}{6} \right) \boldsymbol{\chi}_s \cdot \boldsymbol{\chi}_a + \left(-\frac{27}{16} - \frac{\delta^4}{12} + \frac{\eta}{12} \right) \boldsymbol{\chi}_s^2 \right].$$
$$x^3\left[\frac{167644780815461}{8592292380672} + \left(-\frac{11327099812895}{306867585024} - \frac{205\,\pi^2}{96} \right)\eta - \frac{137763118975\,\eta^2}{1217728512} + \frac{2435519695\,\eta^3}{130470912} \right.$$
$$+ \left(-\frac{21\,\pi}{64} + \frac{275\,\pi\,\delta}{12} + \frac{21\,\pi\,\eta}{16} \right) \boldsymbol{\chi}_a \cdot \hat{\mathbf{L}}_N + \left(\frac{32394371}{2838528} + \frac{791\,\delta}{768} + \frac{113\,\eta^2}{576} + \left(-\frac{71832779}{709632} - \frac{791\,\delta}{192} \right)\eta + \frac{59317\,\eta^2}{264} \right) \boldsymbol{\chi}_a^2 .$$
$$+ \left\{ \frac{275\,\pi}{12} - \frac{21\,\pi\,\delta^3}{64} - \frac{91\,\pi\,\eta}{3} + \left(\frac{791}{768} + \frac{11114513\,\delta}{473088} - \frac{743\,\delta^3}{2688} + \frac{791\,\delta^4}{768} + \left(-\frac{77}{16} - \frac{649327\,\delta}{16896} - \frac{11\,\delta^3}{32} \right)\eta \right.$$
$$\left. \left. + \frac{133\,\eta^2}{48} \right) \boldsymbol{\chi}_a \cdot \hat{\mathbf{L}}_N \right\} \boldsymbol{\chi}_s \cdot \hat{\mathbf{L}}_N + \left(\frac{11114513}{946176} + \frac{791\,\delta^3}{768} - \frac{743\,\delta^4}{5376} + \left(\frac{2007451}{118272} - \frac{133\,\delta^3}{192} - \frac{11\,\delta^4}{64} \right)\eta - \frac{82411\,\eta^2}{2816} \right) \boldsymbol{\chi}_s \cdot \hat{\mathbf{L}}_N \right] \right\} \tag{2.19b}$$

$$\hat{H}_{60} = -\alpha \frac{4195}{1419264\sqrt{273}} x \left\{ 1 - \frac{3612\,\eta}{839} + x\left[-\frac{45661561}{6342840} + \frac{101414\,\eta}{2517} - \frac{48118\,\eta^2}{839} \right] + x^{3/2}\left[\frac{1248\,\pi}{839} - \frac{4992\,\pi\,\eta}{839} \right. \right.$$
$$+ \left(-\frac{44}{5873} + \frac{14129\,\delta}{2517} + \left(\frac{264}{5873} - \frac{140148\,\delta}{5873} \right)\eta - \frac{352\,\eta^2}{5873} \right) \boldsymbol{\chi}_a \cdot \hat{\mathbf{L}}_N + \left(\frac{14129}{2517} - \frac{44\,\delta^3}{5873} \right.$$
$$\left. + \left(-\frac{79120}{2517} + \frac{88\,\delta^3}{5873} \right)\eta + \frac{161136\,\eta^2}{5873} \right) \boldsymbol{\chi}_s \cdot \hat{\mathbf{L}}_N \Big] + x^{5/2}\left[\frac{66616409\,\pi}{2718360} - \frac{874693\,\pi\,\eta}{7551} + \frac{239134\,\pi\,\eta^2}{2517} + \right.$$
$$\left(-\frac{8173}{634248} - \frac{1240441999\,\delta}{57085560} + \left(\frac{6479}{105714} + \frac{15116383\,\delta}{105714} \right)\eta + \left(-\frac{1100}{158571} - \frac{2406356\,\delta}{7551} \right)\eta^2 - \frac{968\,\eta^3}{7551} \right) \boldsymbol{\chi}_a \cdot \hat{\mathbf{L}}_N$$
$$\left. \left(-\frac{1240441999}{57085560} - \frac{8173\,\delta^3}{634284} + \left(\frac{2016684797}{14271390} + \frac{3091\,\delta^3}{317142} \right)\eta + \left(-\frac{19243010}{52857} + \frac{242\,\delta^3}{7551} \right)\eta^2 + \frac{1891144\,\eta^3}{7551} \right) \boldsymbol{\chi}_s \cdot \hat{\mathbf{L}}_N \right]$$
$$x^2\left[\frac{33133408041593}{1594133291520} - \frac{912563795039\,\eta}{25102880} + \frac{8054229309\,\eta^2}{25102880} - \frac{1363643519\,\eta^3}{18827160} + \left(-\frac{81}{32} + \frac{140263\,\eta}{6712} - \frac{36120\,\eta^3}{839} \right) \boldsymbol{\chi}_a^2 \right.$$
$$\left. \left. + \left(-\frac{81\,\delta}{16} + \frac{73143\,\delta\,\eta}{3356} \right) \boldsymbol{\chi}_s \cdot \boldsymbol{\chi}_a + \left(-\frac{81}{32} + \frac{36991\,\eta}{3356} - \frac{7047\,\eta^2}{1678} \right) \boldsymbol{\chi}_s^2 \right] \right. \tag{2.19c}$$

$$\hat{H}_{80} = \alpha \frac{75601}{213497856\sqrt{119}} x^2 \left[1 - \frac{452070\,\eta}{75601} + \frac{733320\,\eta^2}{75601} + x\left(-\frac{265354303}{33869248} + \frac{18177343651\,\eta}{321757856} - \frac{5057483259\,\eta^2}{40219732} + \frac{1828935981\,\eta^3}{20109866} \right) \right] \tag{2.19d}$$

$$\hat{H}_{100} = -\alpha \frac{525221\,x^3}{6452379648\sqrt{154}} \left(1 - \frac{79841784\,\eta}{9979199} + \frac{198570240\,\eta^2}{9979199} - \frac{172307520\,\eta^3}{9979199} \right) \tag{2.19e}$$

We can see that all contribution to $m = 0$, even-l modes arise solely from the Christodoulou memory piece of U_{lm}. There are no hereditary-memory contribution to the radiative current multipole moments V_{lm}

We can combine the above with equation 2.1 and explicitly compute the memory contribution to the + waveform polarization.This can be done in the following way

$$h_{+,\times} = \frac{2\eta M x}{R} H_{+,\times} + O\left(\frac{1}{R^2} \right) \tag{2.20}$$

$$H_{+,\times} = \sum_{n=0}^{\infty} x^{n/2} H_{+,\times}^{(n/2)} \tag{2.21}$$

The memory contribution to $H_+^{n/2}$ are:

$$H_+^{(0,mem)} = \alpha \frac{1}{96} s_\Theta^2 \left(17 + c_\Theta^2\right), \tag{2.22a}$$

$$H_+^{(0.5,mem)} = 0, \tag{2.22b}$$

$$H_+^{(1,mem)} = \alpha s_\Theta^2 \left[-\frac{354241}{2064384} - \frac{62059}{1032192} c_\Theta^2 - \frac{4195}{688128} c_\Theta^4 + \eta\left(\frac{15607}{73728} + \frac{9373}{36864} c_\Theta^2 + \frac{215}{8192} c_\Theta^4\right)\right], \tag{2.22c}$$

$$\begin{aligned} H_+^{(1.5,mem)} = \alpha s_\Theta^2 \Bigg\{ & \left[\frac{3}{1280} + \frac{7}{3840} c_\Theta^2 + \delta\left(\frac{153}{320} + \frac{9}{320} c_\Theta^2\right) + \eta\left(-\frac{3}{320} - \frac{7}{960} c_\Theta^2\right)\right] \boldsymbol{\chi}_a \cdot \hat{\mathbf{L}}_N \\ & + \left[\left(\frac{153}{320} + \frac{9}{320} c_\Theta^2\right) + \delta\left(\frac{3}{1280} + \frac{7}{3840} c_\Theta^2\right) + \eta\left(-\frac{3}{80} + \frac{23}{240} c_\Theta^2\right) + \delta\eta\left(-\frac{3}{320} - \frac{7}{960}\right)\right] \boldsymbol{\chi}_s \cdot \hat{\mathbf{L}}_N \Bigg\} \end{aligned} \tag{2.22d}$$

$$\begin{aligned} H_+^{(2,mem)} = \alpha s_\Theta^2 \Bigg\{ & -\frac{3968456539}{9364045824} + \frac{570408173}{4682022912} c_\Theta^2 + \frac{122166887}{3121348608} c_\Theta^4 + \frac{7560}{15925248} c_\Theta^6 \\ & + \eta\left[-\frac{7169749}{18579456} - \frac{13220477}{18579456} c_\Theta^2 - \frac{1345405}{6193152} c_\Theta^4 - \frac{25115}{884736} c_\Theta^6\right] + \eta^2\left[\frac{10097}{147456} + \frac{5179}{36864} c_\Theta^2 + \frac{44765}{147456} c_\Theta^4\right. \\ & \left. + \frac{3395}{73728} c_\Theta^6\right] + \left[-\frac{1385}{4608} - \frac{85}{4608} c_\Theta^2 + \eta\left(\frac{19}{16} + \frac{7}{96} c_\Theta^2\right)\right] \boldsymbol{\chi}_a^2 + \left[-\frac{1385\sqrt{1-4\eta}}{2304} - \frac{85\sqrt{1-4\eta}}{2304} c_\Theta^2\right. \\ & \left. + \eta\left(\frac{\sqrt{1-4\eta}}{72} + \frac{\sqrt{1-4\eta}}{144} c_\Theta^2\right)\right] \boldsymbol{\chi}_s \cdot \boldsymbol{\chi}_a + \left[-\frac{1385}{4608} - \frac{85}{4608} c_\Theta^2 + \eta^2\left(-\frac{1}{36} - \frac{c_\Theta^2}{72}\right) + \eta\left(\frac{11}{384} + \frac{c_\Theta^2}{128}\right)\right] \boldsymbol{\chi}_s^2 \Bigg\} \end{aligned} \tag{2.22e}$$

$$\begin{aligned} H_+^{(2.5,mem)} = \alpha s_\Theta^2 \Bigg\{ & -\frac{2545\pi}{21504} - \frac{295\pi}{2688} c_\Theta^2 - \frac{65\pi}{7168} c_\Theta^4 + \eta\left[\frac{2545\pi}{5376} + \frac{295\pi}{672} c_\Theta^2 + \frac{65\pi}{1792} c_\Theta^4\right] + \left[\frac{11867}{3612672} + \frac{8156279\sqrt{1-4\eta}}{4816896}\right. \\ & \left. + \frac{163}{112896} c_\Theta^2 - \frac{484979\sqrt{1-4\eta}}{2408448} c_\Theta^2 + \frac{55}{1204224} c_\Theta^4 - \frac{70645\sqrt{1-4\eta}}{2064384} c_\Theta^4 + \eta^2\left(-\frac{3797}{150528} - \frac{411}{25088} c_\Theta^2\right.\right. \\ & \left.\left. + \frac{55}{150528} c_\Theta^4\right) + \eta^2\left(-\frac{3797}{150528} - \frac{411}{25088} c_\Theta^2 + \frac{55}{150528} c_\Theta^4\right) + \eta\left(-\frac{12343}{1806336} - \frac{4105391\sqrt{1-4\eta}}{10838016} - \frac{1517}{903168} c_\Theta^2\right.\right. \\ & \left.\left. + \frac{7446571\sqrt{1-4\eta}}{5419008} - \frac{55}{200704} c_\Theta^4 + \frac{58395\sqrt{1-4\eta}}{401408} c_\Theta^4\right)\right] \boldsymbol{\chi}_a \cdot \hat{\mathbf{L}}_N + \left[\frac{8156279}{4816896} + \frac{11867\sqrt{1-4\eta}}{3612672} + \frac{484979}{2408448} c_\Theta^2\right. \\ & \left. + \frac{163\sqrt{1-4\eta}}{112896} c_\Theta^2 - \frac{70645}{2064384} c_\Theta^4 + \frac{55\sqrt{1-4\eta}}{1204224} c_\Theta^4 + \eta\left(-\frac{7272431}{2709504} - \frac{12343\sqrt{1-4\eta}}{1806336} + \frac{2001211 c_\Theta^2}{1354752}\right.\right. \\ & \left.\left. - \frac{1517\sqrt{1-4\eta}}{903168} c_\Theta^2 + \frac{24725}{129024} c_\Theta^4 - \frac{55\sqrt{1-4\eta}}{200704} c_\Theta^4\right) + \eta^2\left(\frac{1965709}{2709504} - \frac{3797\sqrt{1-4\eta}}{150528} - \frac{1072289}{1354752} c_\Theta^2\right.\right. \\ & \left.\left. - \frac{411\sqrt{1-4\eta}}{25088} c_\Theta^2 - \frac{16785}{100325} c_\Theta^4 + \frac{55\sqrt{1-4\eta}}{150528} c_\Theta^4\right)\right] \boldsymbol{\chi}_s \cdot \hat{\mathbf{L}}_N \Bigg\} \end{aligned} \tag{2.22f}$$

$$\begin{aligned} H_+^{(3,mem)} = \alpha s_\Theta^2 \Bigg\{ & -\frac{69549014242469}{46146017820672} + \frac{6093995955001}{23073008910336} c_\Theta^2 - \frac{1416977186081}{15382005940224} c_\Theta^4 - \frac{2455652411}{78479622144} c_\Theta^6 - \frac{9979199}{2491416576} c_\Theta^8 \\ & + \eta^2\left[\frac{111707903}{594542592} - \frac{792654827}{3269984256} c_\Theta^2 - \frac{9226880251}{6539968512} c_\Theta^4 - \frac{71269747}{148635648} c_\Theta^6 - \frac{7835}{98304} c_\Theta^8\right] + \eta\left[\frac{1355497792045}{149824733184}\right. \\ & \left. - \frac{3485\pi^2}{9216} - \frac{41463325921}{51502252032} c_\Theta^2 - \frac{205\pi^2}{9216} + \frac{347235904277}{549357355008} c_\Theta^4 + \frac{788232313}{3567255552} c_\Theta^6 + \frac{302431}{9437184} c_\Theta^8\right] + \eta^3\left[\frac{10034527}{445906944}\right. \end{aligned}$$

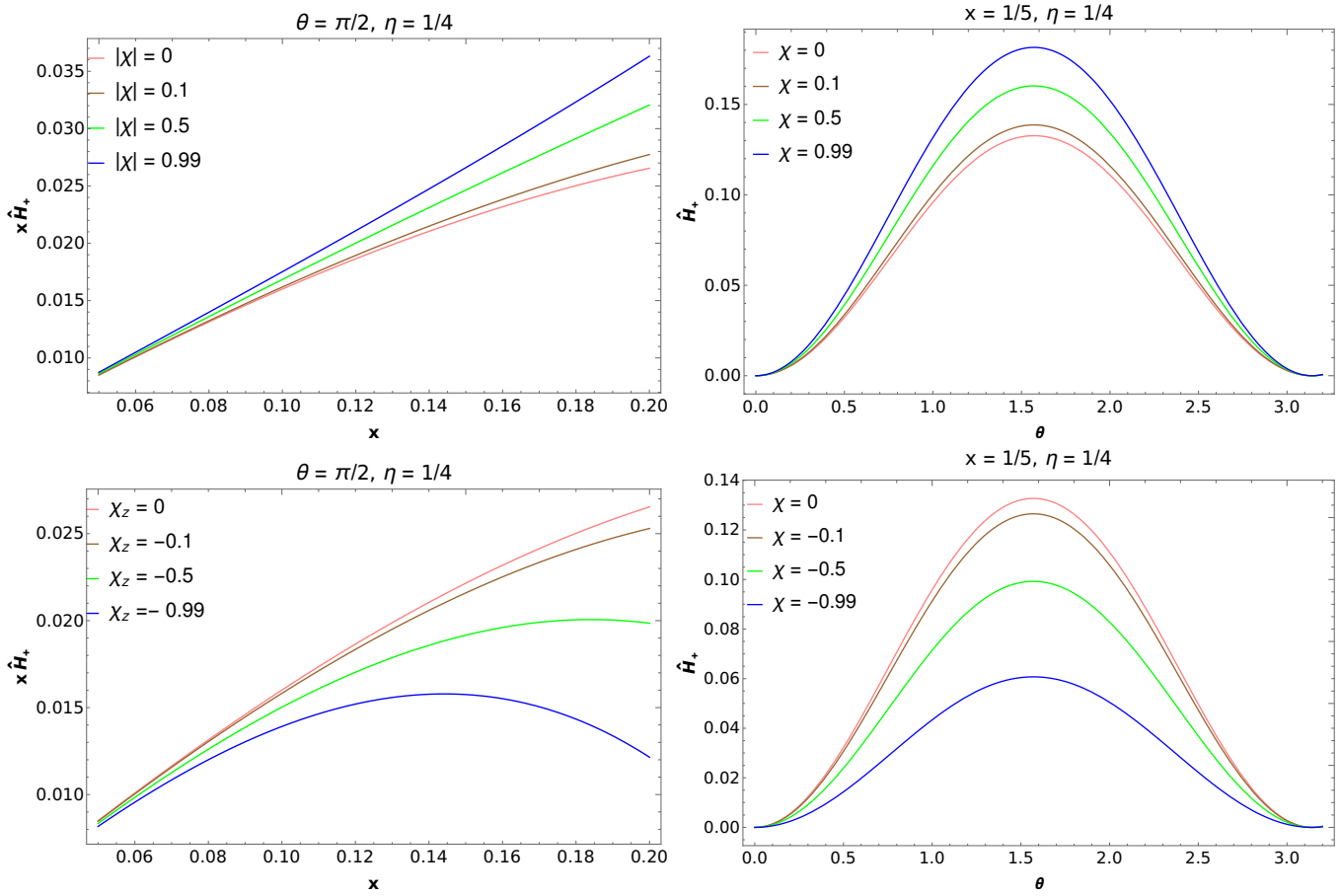

FIG. 1: Dependence of post-Newtonian (PN) corrections to the Christodoulou memory on the binary inclination and orbital separation. The plots above show the memory contribution to H_+ for different dimensionless spin parameter χ values (the polar angle to the observer at = 0 points along the binary orbital angular momentum) for $x = 1/5$ and $\eta = 1/4$. The plot to the right shows xH_+ as a function of parameter x. Increasing the magnitude of does not change the angular dependence, but does tend to increase the magnitude of the memory.

$$+\frac{57932071}{1226244096}c_\Theta^2+\frac{29847079}{544997376}c_\Theta^4+\frac{8170691}{24772608}c_\Theta^6+\frac{9065}{131072}c_\Theta^8\Bigg]+\Bigg[-\frac{14443855}{66060288}+\frac{113\sqrt{1-4\eta}}{8192}+\frac{3716075}{33030144}c_\Theta^2$$
$$+\frac{791\sqrt{1-4\eta}}{73728}+\frac{113265}{7340032}c_\Theta^4+\eta\left(\frac{32497919}{16515072}-\frac{113\sqrt{1-4\eta}}{2048}\right)\Bigg] \tag{2.22g}$$

III. MEMORY CALCULATION USING NUMERICAL RELATIVITY DATA

Numerical relativity simulations most commonly output the Newman-Penrose curvature component ψ_4.The two polarization states, h_+ and $h_\times$ of the gravitational wave are related to the curvature, expressed in terms of the complex Newman-Penrose scalar ψ_4 by

$$\psi_4 = \ddot{h}_+ - i\ddot{h}_\times \tag{3.1}$$

Given the Newman-Penrose scalar ψ_4 for a particular mode, we have to integrate twice in time to obtain h_+ and $h_\times$. It has long been noted that producing a strain, h, from the Newman-Penrose curvature component, ψ_4, typically results in a waveform with unphysical secular non-linear drift [18]. The nonlinearity of drift indicates that this is not simply a result of two constants of integration involved in transformation. This nonlinearity is potentially caused by the fact that ψ_4 is typically extracted at a finite distance from the gravitating source. The strain h is only related to ψ_4 at an infinite distance and also strictly valid in a particular gauge. As a result in numerical simulation, the finite distance calculation introduces a systematic error. In simulations [19, 20], which can possibly extract truly gauge-invariant waveform at future null infinity has not able able to get rid of the secular nonlinear drift.

It has been argued in ref. [13] that an important source of unphysical non-linear drift in numerical computation of gravitational wave strain lies in the transformation of the measured data to the strain h which generally involves an integration in time. The out-

put of the numerical simulation is a discretely sampled time series of finite duration, incorporating some component of unresolved frequencies due to numerical error. This can lead to an uncontrollable non-linear drift if the integration is performed in the time domain. The method described in ref [13] gives us a way to get rid of this unphysical behavior by eliminating the lower frequencies.

The memory contribution to h_+ is given by [14]

$$h_+^{(mem)} \approx \frac{R}{192\,\pi} s_\Theta^2 \left(17 + c_\Theta^2\right) \int_{-\infty}^{T_R} |\dot{h}_{22}|^2 dt \tag{3.2}$$

The above equation requires a time integration of absolute value of $\dot{h}_{22}$, but this is not typically the quantity which is directly computed in numerical simulation. The output of numerical simulation is usually in the form of component of curvature tensor, or Zerilli-Moncrief-type variables defined relative to a background.

A. Evaluating Bondi News from numerical data

The Bondi News which also the first derivative of gravitational wave strain is defined as

$$\mathcal{N} = \int_{-\infty}^{t} dt' \psi_4 \tag{3.3}$$

The gravitational wave memory contribution to h_+ polarization can be computed from this bondi news, by integrating the absolute value of bondi news as shown in equation 3.2. The memory contribution evaluated using Eq.3.2 will contain contribution from numerical noise, which is unphysical and must be removed from the data. We apply the method described in the following section to remove the unphysical part of GW memory.

B. Integration of finite length signals in frequency domain

The unphysical part of mermory essentially lies in lower frequency. A method to remove this unphysical part is given in ref [13]. If we remove this low frequency part from data such that the physical memory is still preserved, we can get rid of memory contribution due to numerical noise. Consider the Fourier transform, $\mathcal{F}$, applied to an absolutely integrable function $f(t)$,

$$\tilde{f}(\omega) = \mathcal{F}[f] = \int_{-\infty}^{\infty} \mathrm{e}^{-\iota\omega t} f(t) dt. \tag{3.4}$$

The Fourier transform of the time integral is given by

$$\mathcal{F}\left[\int_{-\infty}^{t} dt' f(t')\right]|_\omega = -\iota \frac{\tilde{f}(\omega)}{\omega} \tag{3.5}$$

The inverse fourier transform of above expression is given by

$$\int_{-\infty}^{t} dt' f(t') = \mathcal{F}^{-1}\left[-i\frac{\tilde{f}(\omega)}{\omega}\right] = -\frac{i}{2\pi}\int_{-\infty}^{\infty} \frac{1}{\omega} e^{i\omega t} \tilde{f}(\omega) d\omega \tag{3.6}$$

In the frequency-domain, time integration becomes a simple division by the frequency. Above method is particularly susceptible to low-frequency error, under-resolved high-frequency modes can be aliased into low-frequency modes of the signal. We try to remove these unphysical frequencies by the method described below

1. *Fixed frequency integration (FFI)*

The effect of the spurious low-frequency modes caused by spectral leakage or aliasing effects, can be significantly suppressed by use of signal filter. The time integral can be performed in frequency domain as shown in equation 3.6. The low frequencies which cause the unphysical nonlinear drift can be removed by choosing a cutoff frequency while taking a Fourier transform.

$$\tilde{F} = \begin{cases} -i\frac{\tilde{f}(\omega)}{\omega_0} & \omega \le \omega_0 \\ -i\frac{\tilde{f}(\omega)}{\omega} & \omega > \omega_0 \end{cases}$$

We use this method to integrate ψ to obtain Bondi News as shown in equation 3.3.

C. Memory calculation from SXS Rumerical Relativity data

The publicly available SXS catalog provides data for Newman-Penrose scalar component ψ_4, decomposed into spin weighted spherical harmonics, extrapolated to infinite radius. We used this data and performed a frequency domain time integration as described in equation 3.6, while removing the unphysical frequency by choosing a lower cutoff as show in section III B 1. The cutoff frequency is chosen as $\omega_0/10$ where ω_0 is the instantaneous GW angular frequency. We first begin by separating the complex Newman-Perose scalar ψ_4 data into phase and amplitude part. We compute instantaneous GW angular frequency from this by taking the first time derivative of phase corresponding to ψ_4. The instantaneous GW frequency often looks noisy at the beginning of the simulations due to numerical issues. We remove this noise data by choosing a lower and upper cutoff time. Once we find the upper and lower cutoff time, we can apply a frequency domain time integration for ψ_4 by choosing a cutoff frequency. After filtering the noise creating frequency we can use equation 3.2 to compute the memory contribution to "plus" polarization of GW signal. The SXS catalog gives data for different parameter values like mass ratio, dimensionless spin parameter etc. The Christodoulou memory computed from Numerical Relativity data starts from zeros using equation 3.2 due to finite simulation time. Chrostodoulou memory is hereditary, hence it's entire past should be included. This can be done by combining the PN expression during early inspiral and numerical relativity results for merger part. The method used to connect the memory accumulated during entire life time of BBH coalesce is described in the next section.

D. Compleate Christodoulou memory during BBH coalescence

The PN waveform are given as a function of parameter x which is related to time by equation 2.14. This equation can be integrated to obtain a relation between time t and parameter x. The Christodoulou memory reaches it's peak value at the merger. We choose the values of integration constants such that the peak in $h_+^{(mem)}$ is reached at time $t = 0$. For comparison we show the time derivative of $h_+^{(mem)}$ from Numerically obtained results and the analytical expressions in figure 2. The slope as seen from

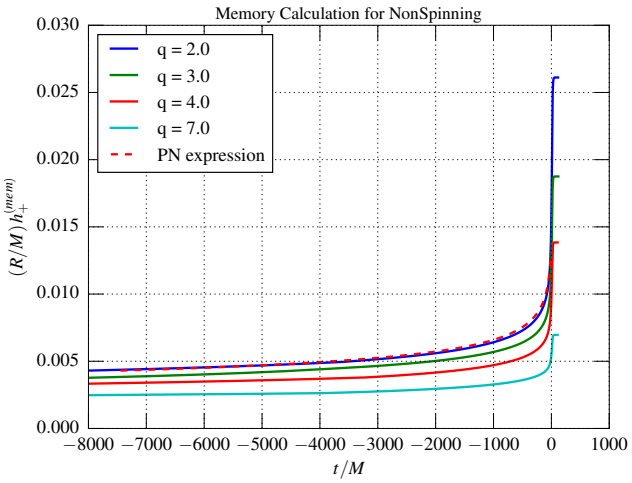

FIG. 2: The figure above shows Christodoulou memory as a function of time during BBH coalesce. This figure shows a comparison for different mass ratios. It can be seen that higher mass ration tends to decrease the Chistodoulou memory. The early inspiral part is computed using post-Newtonian expression and the later part during BBH merger is computer using Numerical Relativity data. The red dashed line shows result from PN expression

figure 2 rises asymptotically. We use our PN results for computing the memory during early inspiral and attach them to NR results. We compare this memory for different mass ratio and different values of dimensionless spin parameter. Figure 3 show the Christodoulou memory for different mass ratios, which shows that the Christodoulou tends to decrease with higher mass ration. The effect of dimensionless spin is shown in figure 4. It can be seen that the spin magnitude has significant effect on nonlinear memory, higher spin magnitude, in case of spin aligned with orbital angular momentum tends to increase the memory contribution. When the spins are anti aligned with orbital angular momentum, the memory tend to decrease the Christodoulou memory. These results show it important to consider the spin contribution when studying the Christodoulou memory in gravitational wave signals.

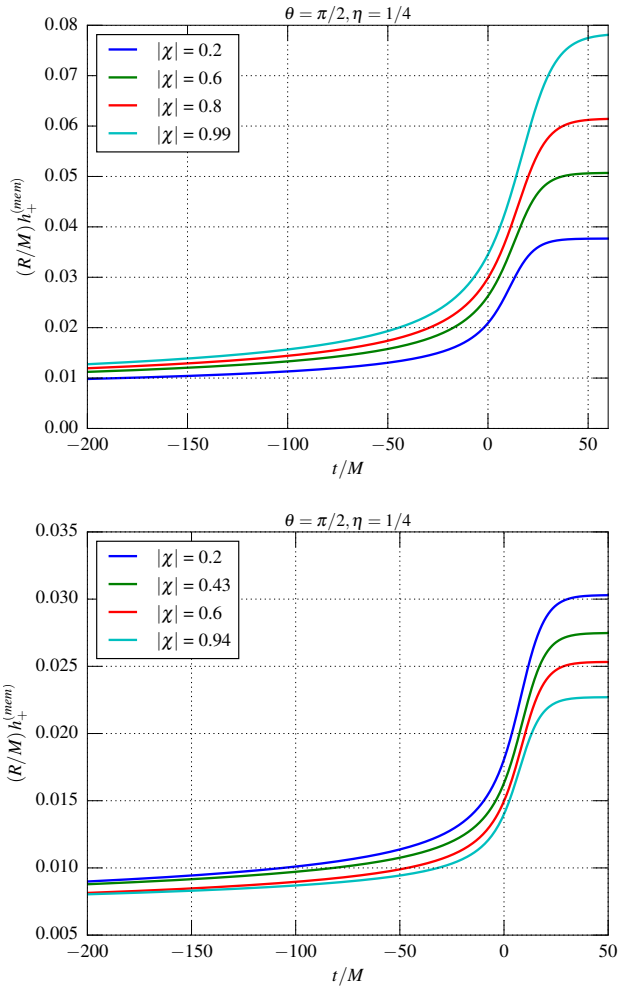

FIG. 3: The figure above shows Christodoulou memory as a function of time during BBH coalesce. The top figure shows a comparison for different values of dimensionless spin parameter χ. These results are for BBH system with equal spin magnitude for individual black hole and spins aligned with orbital angular momentum. It can be seen that higher spin magnitude tend to increase the Christodoulou memory. The bottom figure shows the anti aligned case.

Appendix A: Angular Integral Of The Triple Product Of Spin-Weighted Spherical Harmonics

The following integral appears in the evaluation of nonlinear memory contribution to the radiative mass-multipole moments U_{lm}. Equation 2.4 can be rewritten as

$$d^{l_j}_{m_j s_j}(\Theta) = \sum_{k_j=k_i(j)}^{k_f(j)} g_j(k_j) \left(\sin\frac{\Theta}{2}\right)^{p_j} \left(\cos\frac{\Theta}{2}\right)^{2l_j-p_j} \tag{A1}$$

where

$$g_j(k_j) = \frac{(-1)^k_j[(l_j+m_j)!(l_j-m_j)!(l_j+s_j)!(l_j-s_j)!]^{1/2}}{k_j!(l_j+m_j-k_j)!(l_j-s_j-k_j)!(s_j-m_j+k_j)!}, \tag{A2}$$

$p_j = 2k_j + s_j - m_j$, $k_i = \max(0, m - s)$ and $k_f = \min(l + m, l - s)$. The index $j = 1, 2, 3$ serves only the three harmonics. The required integral can be written as:

$$\begin{aligned} G^{s_1 s_2 s_3}_{l_1 l_2 l_3 m_1 m_2 m_3} &\equiv \int {}_{-s1}Y^{l_1 m_1}(\Theta,\Phi)\,{}_{-s2}Y^{l_2 m_2}(\Theta,\Phi)\,{}_{-s3}Y^{l_3 m_3}(\Theta,\Phi)d\Omega \\ &= (-1)^{s_1+s_2+s_3}\frac{[(2l_1+1)(2l_2+1)(2l_3+1)]^{1/2}}{(4\pi)^{3/2}}\int_0^{2\pi} e^{i(m_1+m_2+m_3)\Phi}d\Phi\int_0^{\pi} d^{l_1}_{m_1 s_1}d^{l_2}_{m_2 s_2}d^{l_3}_{m_3 s_3}\sin(\Theta)d\Theta \end{aligned} \tag{A3}$$

The Φ integral is

$$\int_0^{2\pi} e^{i(m_1+m_2+m_3)\Phi}d\Phi = 2\pi\delta^{-m_1}_{m_2+m_3} \tag{A4}$$

The Φ integral can be written as

$$\int_0^{\pi} d^{l_1}_{m_1 s_1}d^{l_2}_{m_2 s_2}d^{l_3}_{m_3 s_3}\sin\Theta d\Theta = 2\sum_{k_1 k_2 k_3} g_1(k_1)g_2(k_2)g_3(k_3)\int_0^{\pi}\left(\sin\frac{\Theta}{2}\right)^{2a-1}\left(\cos\frac{\Theta}{2}\right)^{2b-1}d\Theta \tag{A5}$$

where $a = 1 + (p_1 + p_2 + p_3)/2$ and $b = 1 + l_1 + l_2 + l_3 - (p_1 + p_2 + p_3)/2$. The Φ integral is expression in terms of the Beta or Gamma function and can be found in standard tables.

$$\int_0^{\pi}\left(\sin\frac{\Theta}{2}\right)^{2a-1}\left(\cos\frac{\Theta}{2}\right)^{2b-1}d\Theta = \frac{\Gamma(a)\Gamma(b)}{\Gamma(a+b)} = B(a,b) \tag{A6}$$

Appendix B: Calculation Of The $\dot{h}_{lm}$ Modes

The h_{lm} modes are written as

$$h_{lm} = 8\sqrt{\frac{\pi}{5}}\frac{\eta M}{R}x\hat{H}_{lm}(x)e^{im\psi} \tag{B1}$$

where the $\hat{H}_{lm}$ are obtained by taking the non-precessing limit of expressions for precessing binaries given in Ref.[15] . In this paper we are interested in nonprecessing case, so we rewrite the expressions such that spin are aligned with the total orbital angular momentum. The phase variable ψ is related to the orbital phase ϕ via

$$\psi = \varphi - 3x^{3/2}\left[1 - \frac{\eta}{2}x\right]\ln\left(\frac{x}{x_0}\right) \tag{B2}$$

where $\ln x_0 = \frac{11}{18} - \frac{2}{3}\gamma_E - \frac{4}{3}\ln 2 + \frac{2}{3}\ln\left(\frac{M}{r_0}\right)$ is related to the arbitrary constant r_0 appearing in the coordinate transformation of Eq. (2.20) or ref[12]. The orbital phase can be expressed a function of x for nonprecessing binaries, to 3.5PN order.This expression is given in Eq(3.4) of Ref. [21]

$$\begin{aligned} \varphi(x) = -\frac{1}{32\,\eta\,x^{5/2}}\Bigg\{ & 1 + x\left[\frac{55\eta}{12} + \frac{3715}{1008}\right] + x^{3/2}\left[\frac{565}{24}\left(\left(1 - \frac{76\eta}{133}\right)\boldsymbol{\chi}_s\cdot\hat{\mathbf{L}}_N + \delta\boldsymbol{\chi}_a\cdot\hat{\mathbf{L}}_N\right) - 10\pi\right] \\ & + x^2\left[\left(\boldsymbol{\chi}_a\cdot\hat{\mathbf{L}}_N\right)^2\left(150\eta - \frac{3595}{96}\right) - \frac{3595\boldsymbol{\chi}_a\cdot\hat{\mathbf{L}}_N\boldsymbol{\chi}_s\cdot\hat{\mathbf{L}}_N\delta}{48} + \boldsymbol{\chi}_a^2\left(\frac{1165}{96} - 50\eta\right) + \frac{1165\boldsymbol{\chi}_s\cdot\boldsymbol{\chi}_a\delta}{\delta}\right] \\ & + \left(\boldsymbol{\chi}_s\cdot\hat{\mathbf{L}}_N\right)^2\left(-\frac{5\eta}{24} - \frac{3595}{96}\right) + \boldsymbol{\chi}_s^2\left(\frac{35\eta}{24} + \frac{1165}{96}\right) + \frac{3085\eta^2}{144} + \frac{27145\eta}{1008} + \frac{15293365}{10160664}\Bigg] \\ & + \frac{x^{5/2}}{2}\left[\left(\boldsymbol{\chi}_a\cdot\hat{\mathbf{L}}_N\left(-\frac{35\delta\eta}{2} - \frac{732985\delta}{2016}\right) + \boldsymbol{\chi}_s\cdot\hat{\mathbf{L}}_N\left(\frac{85\eta^2}{2} + \frac{6065\eta}{18} - \frac{732985}{2016}\right) - \frac{65\pi\eta}{8} + \frac{38645\pi}{672}\right)\ln(x)\right] \\ & x^3\left[-\frac{127825\eta^3}{5184} + \frac{76055\eta^2}{6912} + \frac{2255\pi^2\eta}{48} - \frac{15737765635\eta}{12192768} - \frac{1712\gamma_E}{21} - \frac{160\pi^2}{3} + \frac{12348611916451}{18776862720} - \frac{1712\ln(16x)}{42}\right] \\ & x^{7/2}\left[-\frac{74045\pi\eta^2}{6048} + \frac{378515\pi\eta}{12096} + \frac{77096675\pi}{2032128}\right]\Bigg\} \end{aligned} \tag{B3}$$

where φ_0 is a certain reference phase. The first time derivative of modes can be obtained by using equation B1 and substituting the expression for $\dot{x}$ as a function of x using Eq. C3. We use the expression for time derivative as show in equation below

$$\dot{h}_{lm} = 8\sqrt{\frac{\pi}{5}}\frac{\eta M}{R}\dot{x}e^{-im\psi}\left(\tilde{H}'_{lm} - im\psi'\tilde{H}_{lm}\right) \tag{B4}$$

where the prime denotes the derivative with respect to x.

Appendix C: Complete 3.5 PN expressions for Energy and Flux

$$\begin{aligned}
E = -\frac{\eta M x}{2}\Bigg\{1 + x\left[-\frac{3}{4} - \frac{\eta}{12}\right] + x^{3/2}\left[\left(\frac{8}{3} - \frac{4\eta}{3}\right)\boldsymbol{\chi}_s\cdot\hat{\mathbf{L}}_N + \frac{8}{3}\delta\boldsymbol{\chi}_a\cdot\hat{\mathbf{L}}_N\right] \\
x^2\left[-\frac{27}{8} + \frac{19\eta}{8} - \frac{\eta^2}{24} + \eta^2\left\{\left(\boldsymbol{\chi}_s^2 - \boldsymbol{\chi}_a^2\right) - 3\left[\left(\boldsymbol{\chi}_s\cdot\hat{\mathbf{L}}_N\right)^2 - \left(\boldsymbol{\chi}_a\cdot\hat{\mathbf{L}}_N\right)^2\right]\right\}\right. \\
\left.\left(\frac{1}{2} - \eta\right)\left\{\boldsymbol{\chi}_s^2 + \boldsymbol{\chi}_a^2 - 3\left[\left(\boldsymbol{\chi}_s\cdot\hat{\mathbf{L}}_N\right)^2 + \left(\boldsymbol{\chi}_a\cdot\hat{\mathbf{L}}_N\right)^2\right]\right\} + \delta\left\{\boldsymbol{\chi}_s\cdot\boldsymbol{\chi}_a - 3\left[\left(\boldsymbol{\chi}_s\cdot\hat{\mathbf{L}}_N\boldsymbol{\chi}_s\cdot\hat{\mathbf{L}}_N\right)\right]\right\}\right] \\
x^{5/2}\left[\left(8 - \frac{121\eta}{9} + \frac{2\eta^2}{9}\right)\boldsymbol{\chi}_s\cdot\hat{\mathbf{L}}_N + \left(8 - \frac{31\eta}{9}\right)\delta\boldsymbol{\chi}_a\cdot\hat{\mathbf{L}}_N\right] + x^3\left[-\frac{675}{64} + \left(\frac{34445}{576} - \frac{205\pi^2}{96}\right)\eta - \frac{155\eta^2}{96} - \frac{35\eta^3}{5184}\right]\Bigg]\Bigg\}
\end{aligned} \tag{C1}$$

$$\begin{aligned}
\mathcal{L} = \frac{32}{5}\eta^2 x^5\Bigg\{1 + x\left[-\frac{1247}{336} - \frac{35\eta}{12}\right] + x^{3/2}\left[4\pi - \left\{\left(\frac{11}{4} - 3\eta\right)\boldsymbol{\chi}_s\cdot\hat{\mathbf{L}}_N + \frac{11}{4}\delta\boldsymbol{\chi}_a\cdot\hat{\mathbf{L}}_N\right\}\right] \\
x^2\left[-\frac{44711}{9072} + \frac{9271\eta}{504} + \frac{65\eta^2}{18} + \left(\frac{287}{96} + \frac{\eta}{24}\right)\left(\boldsymbol{\chi}_s\cdot\hat{\mathbf{L}}_N\right)^2 - \left(\frac{89}{96} + \frac{7\eta}{24}\right)\boldsymbol{\chi}_s^2\right. \\
\left. + \left(\frac{287}{96} - 12\eta\right)\left(\boldsymbol{\chi}_a\cdot\hat{\mathbf{L}}_N\right)^2 + \left(-\frac{89}{96} + 4\eta\right)\boldsymbol{\chi}_a^2 + \frac{287}{48}\delta\left(\boldsymbol{\chi}_s\cdot\hat{\mathbf{L}}_N\right)\left(\boldsymbol{\chi}_a\cdot\hat{\mathbf{L}}_N\right) - \frac{89}{48}\delta\left(\boldsymbol{\chi}_s\cdot\boldsymbol{\chi}_a\right)\right] \\
x^{5/2}\left[\left(-\frac{8191}{672} - \frac{583\eta}{24}\right)\pi + \left\{\left(-\frac{59}{16} + \frac{227\eta}{9} - \frac{157\eta^2}{9}\right)\boldsymbol{\chi}_s\cdot\hat{\mathbf{L}}_N + \left(-\frac{59}{16} + \frac{701\eta}{36}\delta\boldsymbol{\chi}_a\cdot\hat{\mathbf{L}}_N\right)\right\}\right] \\
x^3\left[\frac{6643739519}{69854400} + \frac{16\pi^2}{3} - \frac{1712\gamma_E}{105} - \frac{856}{105}\log(16x) + \left(-\frac{134543}{7776} + \frac{41\pi^2}{48}\right)\eta - \frac{94403\eta^2}{3024} - \frac{775\eta^3}{324}\right]\Bigg\}
\end{aligned} \tag{C2}$$

$$\begin{aligned}
\frac{dx}{dt} = \frac{64x^5\eta}{5}\Bigg\{1 + x\left[-\frac{743}{336} - \frac{11\eta}{4}\right] + x^{3/2}\left[4\pi - \frac{113}{12}\delta\boldsymbol{\chi}_a\cdot\hat{\mathbf{L}}_N - \left(-\frac{113}{19} + \frac{19\eta}{3}\right)\boldsymbol{\chi}_s\cdot\hat{\mathbf{L}}_N\right] \\
+ x^2\left[\frac{34103}{18144} + \frac{13661\eta}{2016} + \frac{59\eta^2}{18} + \left(\frac{719}{96} - 30\eta\right)(\boldsymbol{\chi}_a\cdot\hat{\mathbf{L}}_N)^2 + \boldsymbol{\chi}_a^2\left(-\frac{233}{96} + 10\eta\right)\right. \\
\left. + \frac{719\boldsymbol{\chi}_a\cdot\hat{\mathbf{L}}_N\boldsymbol{\chi}_s\cdot\hat{\mathbf{L}}_N\delta}{48} - \frac{233\boldsymbol{\chi}_s\cdot\boldsymbol{\chi}_a\delta}{48} + (\boldsymbol{\chi}_s\cdot\hat{\mathbf{L}}_N)^2\left(-\frac{\eta}{24} - \frac{719}{96}\right) + \boldsymbol{\chi}_s^2\left(\frac{7\eta}{24} + \frac{233}{96}\right)\right] \\
+ x^{5/2}\left[-\frac{4159\pi}{672} - \frac{189\pi\eta}{8} + \boldsymbol{\chi}_a\cdot\hat{\mathbf{L}}_N\delta\left(-\frac{31319}{1008} + \frac{1159\eta}{24}\right) + \boldsymbol{\chi}_s\cdot\hat{\mathbf{L}}_N\left(-\frac{31319}{1008} + \frac{22975\eta}{252} - \frac{79\eta^2}{3}\right)\right] \\
+x^3\left[\frac{16447322263}{139708800} + \frac{16\pi^2}{3} - \frac{1712\gamma_E}{105} - \frac{56198689\eta}{217728} + \frac{451\pi^2\eta}{48} + \frac{541\eta^2}{896} - \frac{5605\eta^3}{2592} - \frac{80\pi\delta\boldsymbol{\chi}_a\cdot\hat{\mathbf{L}}_N}{3}\right. \\
+\left(\frac{575}{448} + \frac{565\delta^2}{9} - \frac{65815\eta}{4032} + \frac{89\eta^2}{2}\right)(\boldsymbol{\chi}_a\cdot\hat{\mathbf{L}}_N)^2 + \left(-\frac{145}{448} + \frac{21985\eta}{4032} - \frac{89\eta^2}{6}\right)\boldsymbol{\chi}_a^2 + \left(-\frac{80\pi}{3} + \frac{40\pi\eta}{3}\right. \\
+\delta\left(\frac{258295}{2016} - \frac{9203\eta}{96}\right)\boldsymbol{\chi}_a\cdot\hat{\mathbf{L}}_N\Big)\boldsymbol{\chi}_s\cdot\hat{\mathbf{L}}_N + \left(\frac{258295}{4032} - \frac{48773\eta}{576} + \frac{3041\eta^2}{144}\right)(\boldsymbol{\chi}_s\cdot\hat{\mathbf{L}}_N)^2 + \delta\left(-\frac{145}{224} + \frac{2143\eta}{288}\right)\boldsymbol{\chi}_s\cdot\boldsymbol{\chi}_a \\
\left.+\left(-\frac{145}{448} + \frac{1891\eta}{576} - \frac{7\eta^2}{144}\right)\boldsymbol{\chi}_s^2 - \frac{3424\ \log[2]}{105} - \frac{1712\log[x]}{210}\right]\Bigg\}
\end{aligned} \tag{C3}$$

References

[1] M. B. Davies, A. King, S. Rosswog, and G. Wynn, Astrophys. J. **579**, L63 (2002), arXiv:astro-ph/0204358 [astro-ph] .

[2] A. Buonanno, G. Sigl, G. G. Raffelt, H.-T. Janka, and E. Müller, Phys. Rev. D **72**, 084001 (2005), arXiv:astro-ph/0412277 [astro-ph] .

[3] K. Kotake, W. Iwakami, N. Ohnishi, and S. Yamada, Astrophys. J. **697**, L133 (2009), arXiv:0904.4300 [astro-ph.HE] .

[4] V. B. Braginskii and K. S. Thorne, Nature (London) **327**, 123 (1987).

[5] D. Christodoulou, Phys. Rev. Lett. **67**, 1486 (1991).

[6] P. N. Payne, Phys. Rev. D **28**, 1894 (1983).

[7] L. Blanchet and T. Damour, Phys. Rev. D **46**, 4304 (1992).

[8] K. S. Thorne, Rev. Mod. Phys. **52**, 299 (1980).

[9] R. A. Isaacson, Phys. Rev. **166**, 1272 (1968).

[10] A. G. Wiseman and C. M. Will, Phys. Rev. D **44**, R2945 (1991).

[11] K. S. Thorne, Phys. Rev. D **45**, 520 (1992).

[12] M. Favata, Phys. Rev. D **80**, 024002 (2009), arXiv:0812.0069 [gr-qc] .

[13] C. Reisswig and D. Pollney, Classical and Quantum Gravity **28**, 195015 (2011), arXiv:1006.1632 [gr-qc] .

[14] M. Favata, Classical and Quantum Gravity **27**, 084036 (2010), arXiv:1003.3486 [gr-qc] .

[15] K. G. Arun, A. Buonanno, G. Faye, and E. Ochsner, Phys. Rev. D **79**, 104023 (2009), arXiv:0810.5336 [gr-qc] .

[16] L. Blanchet, G. Faye, B. R. Iyer, and S. Sinha, Classical and Quantum Gravity **25**, 165003 (2008), arXiv:0802.1249 [gr-qc] .

[17] L. E. Kidder, Phys. Rev. D **77**, 044016 (2008), arXiv:0710.0614 [gr-qc] .

[18] E. Berti, V. Cardoso, J. A. Gonzalez, U. Sperhake, M. Hannam, S. Husa, and B. Brügmann, Phys. Rev. D **76**, 064034 (2007), arXiv:gr-qc/0703053 [gr-qc] .

[19] M. Hannam, S. Husa, J. G. Baker, M. Boyle, B. Brügmann, T. Chu, N. Dorband, F. Herrmann, I. Hinder, B. J. Kelly, L. E. Kidder, P. Laguna, K. D. Matthews, J. R. van Meter, H. P. Pfeiffer, D. Pollney, C. Reisswig, M. A. Scheel, and D. Shoemaker, Phys. Rev. D **79**, 084025 (2009), arXiv:0901.2437 [gr-qc] .

[20] C. Reisswig, N. T. Bishop, D. Pollney, and B. Szilágyi, Phys. Rev. Lett. **103**, 221101 (2009), arXiv:0907.2637 [gr-qc] .

[21] P. Ajith, Phys. Rev. D **84**, 084037 (2011), arXiv:1107.1267 [gr-qc] .